

Hydrodynamics and Eutrophication Modelling for Singapore Straits

P.TKALICH*, PANG W.C. AND P.SUNDARAMBAL
Tropical Marine science Institute, National University of Singapore
**tmspt@nus.edu.sg*

Abstract

Princeton Ocean Model (POM) and eutrophication model (NEUTRO) are utilized to predict hydrodynamics and eutrophication processes in Singapore Straits. Accurate bathymetry of Singapore Straits is computed with the developed 2-D interpolation algorithm. The hydrodynamic modelling strategies with respect to the sloped tidal forcing boundaries, monsoon effect, vertical salinity and temperature stratification are presented. The output of the hydrodynamic model POM is coupled with the input for the water quality model NEUTRO using file interface. NEUTRO considers eleven state variables, including nitrogen, phosphorus, phytoplankton and zooplankton, dissolved oxygen and suspended matter. The baseline concentrations are obtained from the field measurements using statistical analysis. The model is calibrated to reproduce observed dynamics of the nutrients. The hydrodynamics and water quality models can be used to predict impact of coastal development and technogenic spills on marine environment.

Keywords: POM, bathymetry interpolation, tidal forcing, hydrodynamics, eutrophication, plankton dynamics, water quality simulation.

1. INTRODUCTION

Rapid economic development in coastal zones usually involves large-scale land reclamation, construction of port and harbour facilities, and other changes of coastal line, which may cause alteration of local equilibrium circulation patterns. Land reclamation of the Singapore coast has started since the mid-1960s and intensified in the 70s. The reclaimed land modified southern coastline of the mainland, as well as some of offshore islands. Numerical model is the useful tool to predict consequences of coastline changes on circulation currents. Development of numerical hydrodynamic models for Singapore Straits has started since the 90s. Two-dimensional models were developed by Cheong et al. (1992) and also Shankar et al. (1997). In recent years, developments were also made on 3-D hydrodynamic models (Chao et al., 1999; Zhang et al., 2000).

Urbanisation of coastal zones often leads to increase of waste discharge into the aquatic environment. Even though seawater has some natural purification capabilities, extra loading of pollutants may deteriorate the water quality, causing eutrophication and adverse toxic effects on marine ecosystem. The combined effect of pollutant and nutrient load may cause outbreak of harmful algal bloom and loss of natural habitat. There are several commercial and research codes available for eutrophication modelling. WASP eutrophication model (Ambrose et al., 2001) can be

used to analyze a variety of water quality problem in such diverse water bodies as estuaries and coastal waters. The equations implemented in WASP were derived from the Potomac Eutrophication Model, PEM (Thomann and Fitzpatrick et al., 1982), and are fairly standard. WASP is the box-type model, which utilise space-averaged nutrient fluxes instead of three-dimensional advection-diffusion mass transport. Plankton and nutrient concentration depends on variation of light, vertical stratification and current structure of water column; therefore, the box-integrated approach is less accurate compared to the full 3-D models. The influence of these parameters can be significant in the vicinity the shoreline, where surface runoff and freshwater river discharge tend to develop layered structures in the water column.

A number of three-dimensional eutrophication models have been developed for temperate waters. A comprehensive model, developed for the Chesapeake Bay (Carl et al., 1993,1995), couples a water quality module with the three-dimensional hydrodynamics and benthic processes. Ecological North Sea Model Hamberg (ECOHAM1, Andreas, M. 1997) is a 3-D numerical model to quantify the regional productivity on an annual basis. The model utilizes a simple phosphorus cycle, takes into account only two pelagic variables (phytoplankton and phosphate). The three dimensional flow and water quality model (EIA 3D) by Kuusisto et al. (1998) was used to simulate

phytoplankton biomass and dissolved nutrient concentrations in the Gulf of Finland. The model considers 4 state variables like dissolved phosphorus, dissolved nitrogen, total phytoplankton biomass in wet weight and detritus biomass. In the model transport of nutrients is based on calculated wind and river-flow induced currents calculated with the 3-D baroclinic model. To accommodate the spatial and temporal variability, the proficient kinetics of WASP model sometimes is combined with the 3-D advection – diffusion contaminant transport module, as it is done by Gin and Tkalich (1998) in NEUTRO model. This approach was later utilised in Zhang et al's (2000) model.

Current version of NEUTRO takes into account the nitrogen, phosphorus, carbon and silica cycles; phytoplankton and zooplankton dynamics; and dissolved oxygen balance. Advective velocities and eddy viscosity parameters are computed using the Princeton Ocean Model.

2. ACCURATE BATHYMETRY MAP

Due to the intensive reclamation work in Singapore coastal areas, bathymetry map requires constant update. The available data, originally designed for navigation purposes of are often given in the form of irregularly distributed points or contour lines, which have to be interpolated on computational grid to be used in the numerical models. A 2-D interpolation algorithm has been developed to obtain accurate and up-to-date gridded bathymetry of Singapore Straits.

Interpolation technique. The interpolation algorithm utilises 3 irregularly spaced original data points to find the interpolated value in the target point (grid-node). The data points form a triangle which encloses the target point, as shown in Figure 1.

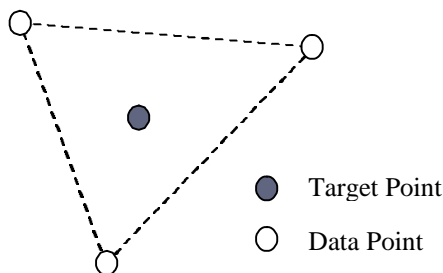


Figure 1. Three data points form a triangle that enclose the target point.

If coordinates $(x, y)_{A,B,C}$ and depth $(z)_{A,B,C}$ of the data points A, B, and C are known, the depth z_T of the target point T with the coordinates $(x, y)_T$ can be obtained by solving the equation of plane

$$\begin{vmatrix} x_T - x_A & y_T - y_A & z_T - z_A \\ x_B - x_A & y_B - y_A & z_B - z_A \\ x_C - x_A & y_C - y_A & z_C - z_A \end{vmatrix} = 0. \quad (1)$$

Simple trigonometry considerations are used to determine whether the 3 points A, B and C enclose the point T, such that if θ_{AB} is the clockwise angle between the line AT and BT, then if $\theta_{AC} > \theta_{AB}$, $\mathbf{q}_{AB} < 180^\circ$ and $\mathbf{q}_{AC} > 180^\circ$ (2) and vice versa.

To make the algorithm more efficient, the original points are grouped according to their geographical location and a distance to the target point. Only data points within the user-defined distance are used for the interpolation. If no set of 3 points satisfy the enclosure of triangle criteria, more groups within a longer distance from the target point are called upon. The process continues until the required 3 points are found or a user-defined maximum range is exceeded. The linear interpolation algorithm is chosen over nonlinear ones because it would always produce reasonable estimation, even in region of highly uneven depths where most nonlinear methods overshoot or undershot. To accommodate bathymetry data of subgrid resolution, such as causeway, narrow channels, bridges, small islands and certain important land geometry, manual node-to-node editing has been applied.

Three sets of data are used for computation of the new bathymetry, namely the Electronic Navigation Chart (ENC) of Singapore, Navigation Chart 202 (1998) by Maritime Port Authority of Singapore (MPA) and MPA's digital map in isoline form. The Navigation Chart 202 (originally in a paper form) was digitised into ASCII format using in-house developed Matlab tools. In total, 550,000 points in Cartesian co-ordinates are obtained.

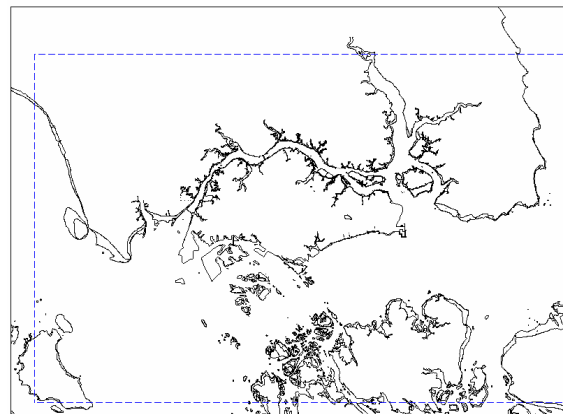


Figure 2. Domain of original data (outer rectangle) and domain of numerical simulation (inner dash-line rectangle)

Figure 2 shows the domain of numerical simulation (enclosed by smaller dash-line rectangle). The domain's size is 110 km east-west and 61 km north-south; and the interpolation grid-size is 250m x 250m, resulting in a total of 50,000 target points. The results are then averaged to obtain the 1km x 1km bathymetry used for test simulation.

Resulting bathymetry map. Figure 3 shows a typical target point (marked by the cross) with 4 enclosing triangles found. Figure 4 is a contour plot of interpolated 250m x 250m resolution grid.

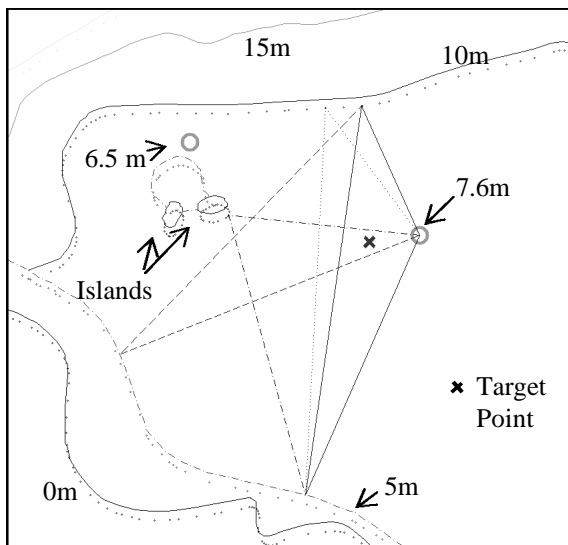


Figure 3. A target point with 4 sets of 3 points (shown as triangles) found.

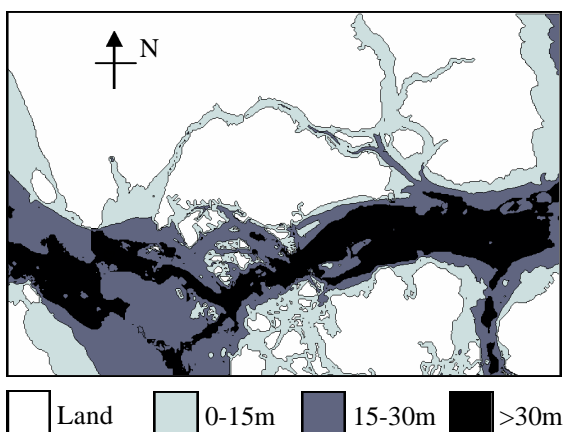


Figure 4. Contour plot of the computed 250m x 250m grid

3. HYDRODYNAMICS SIMULATION

The hydrodynamics of Singapore Straits is simulated using the 3-D Princeton Ocean Model (POM, Blumberg and Mellor, 1987). POM is a 3-D

free surface primitive equation model with a second order turbulence closure model. Originally used for oceanic scale hydrodynamic modelling, the model has in recent years been applied to coastal water problems. The following sections will outline some important features of the Singapore water hydrodynamics and the corresponding modelling strategies.

Tidal currents. Tides in Singapore are the results of tidal generation in the South China Sea and Northern Indian Ocean. Tidal waves are semi-diurnal and travel mainly in the eastern and western directions. Prescribed tidal elevation values at the open boundaries (Figure 5) are used to parameterise the tidal forcing in the model.

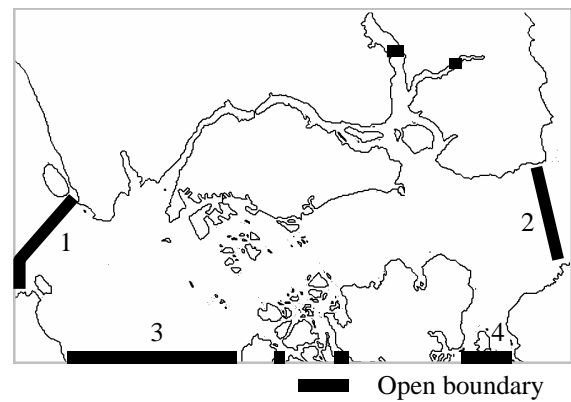


Figure 5. Open boundaries of the hydrodynamic model. The main boundaries are marked with numbers.

To maintain real-time simulation and forecast capabilities, the tidal prediction software TotalTide (http://www.ukho.gov.uk/total_tide.html) is used to satisfy the boundary conditions. The program makes use of harmonic constituents or published data from the authorities of the respective countries (Singapore, Malaysia and Indonesia for our case) for tidal prediction. The harmonic predictions are available only in certain locations (stations); therefore, if a boundary condition is falling between two stations, a linear interpolation of tidal parameters is used. If there is only one station nearby and direction of tidal wave is known, the celerity of tidal wave propagation, C_T , is used for correction

$$C_T = (g \cdot h)^{1/2}, \quad (3)$$

where h is the water depth, g is the gravity acceleration. If direction of tidal wave is unknown or varying, the predicted tidal value of the nearest station is used.

Monsoon influence. The local climate of Singapore Straits is influenced strongly by the Asian monsoon. There are two prevailing monsoon periods in a year – the southwest monsoon from

June to September and the northeast monsoon from November to March. In Singapore Straits the monsoon currents are significant and found to be superimposed on the tidal current, as reported by Tham (1953). The joint tidal studies of 1979 (Indonesia, Japan, Malaysia and Singapore) has found that the average non-tidal streams (presumably monsoon), passing the southern water of Singapore at 10m below water surface, to be around 0.5m/s during the two prevailing monsoons, compared to tidal streams of 0.2-2.5m/s (depending on tidal cycle) at the same location. However, harmonic prediction of TotalTide does not take into account the effect of monsoon, and amount of respective data elsewhere is limited. While numerical modelling of the Australian-Asian monsoon is a possible alternative because the monsoon wind regime is well studied and recorded, it would require a domain much larger than Singapore Straits, which far exceeds the scope and resource of the project. Incorporation of the monsoon constituent would require much more field surveys and modelling efforts.

Water Column: Temperature and Salinity. Field survey of the physical parameters in Singapore Straits has been reported by Zhang and Chan (1999). Vertical distribution of temperature and salinity is varied slightly along the Straits, and is shown in Figure 6 for one of the locations.

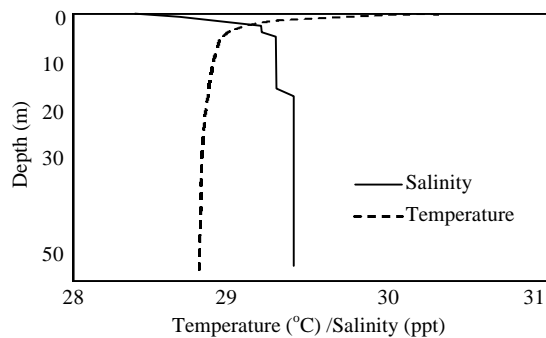


Figure 6. The vertical distribution of temperature and salinity for one of offshore stations in December 1997.

In majority places, the vertical variation of temperature is insignificant. Another field survey, conducted since March 2001 also shows that vertical variation of temperature is usually less than 1°C. On the other hand, vertical variation of salinity can be high along the inshore region of Johor Straits and Pulau Tekong. It is believed that fresh water discharge from rivers and surface runoff can be the contributors.

Considering the dominant hydrodynamics in the offshore region of Singapore Straits, the

simulations presented in this paper are barotropic. Vertical mixing due to salinity stratification will be included at the later stage, as more data become available.

Sloped boundaries vs. vertical boundaries. In the case of rectangular grid for POM, the conventional open boundaries are parallel to x or y co-ordinates. However, such assumption can not be used for Singapore Straits, where the tidal studies of 1979 show sloped co-tidal lines of the major tidal constituents as in Figure 7 and 8. The Figures show co-tidal chart of the dominant M2 and K1+O1 tides as they enter and leave Singapore Straits. The M2, K1 and O1 components contribute more than 60% of the tidal magnitude in Singapore Straits.

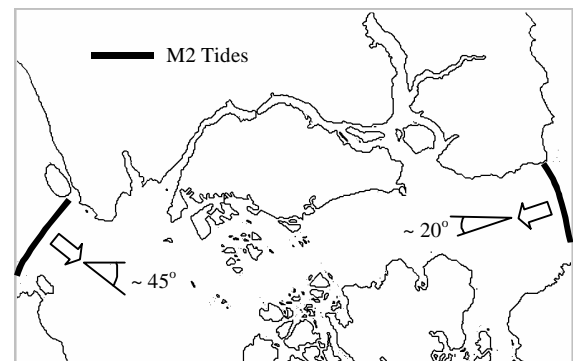


Figure 7. Illustrative co-tidal chart of M2 tidal component.

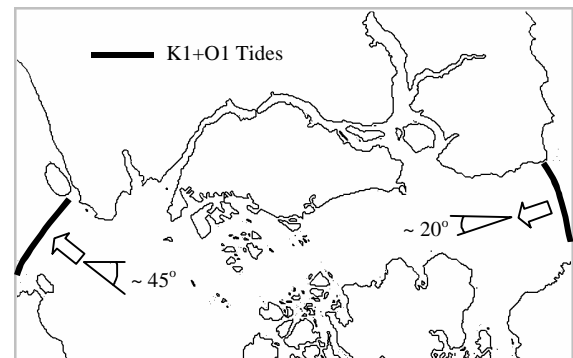


Figure 8. Illustrative co-tidal chart of K1+O1 tidal components.

The tidal streams at the boundaries are expected to travel along the tidal waves, i.e. they also are not parallel to x or y co-ordinates. As such, sloped boundary conditions are used at the western and eastern boundaries with orientation of 45° and 20° respectively.

Simulation results. Simulation was performed for a 7 days period during August 2002 in a dual processor SunBlade 1000 system. The 1kmx1km grid is used with an external time step of 3 seconds.

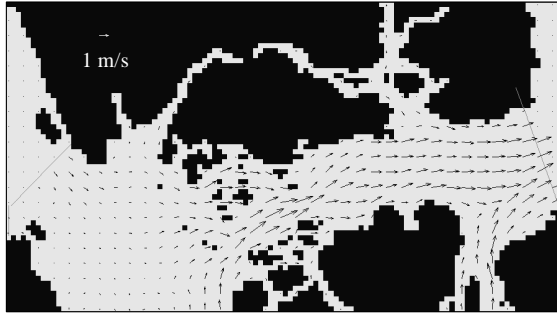


Figure 9. Predicted current ebbing pattern in August 2002.

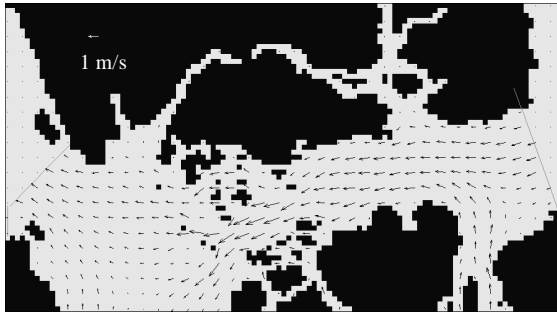


Figure 10. Predicted current flooding pattern in August 2002.

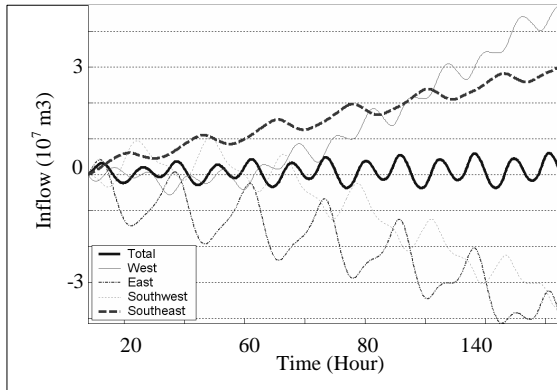


Figure 11. Total inflow (negative for outflow) at the four main boundaries for 7 days.

The predicted tide-induced current ebbing and flooding patterns are shown in Figure 9 and 10. Figure 11 shows the total inflow computed for the four main open boundaries over 7 days. The figure indicates that water comes into Singapore Straits mainly through west and southeast boundaries, and exit through the east and southwest boundaries.

4. EUTROPHICATION MODELLING

Eutrophication Model Structure. The developed eutrophication model (NEUTRO) predicts water quality with respect to nutrients, plankton and dissolved oxygen, as well as bacteria decay and other reactive pollutants in water column. The conceptual framework for the eutrophication

kinetics in the water column is based on the WASP model. Seven interacting system are selected, comprising the nitrogen, phosphorus, carbon and silica cycles; phytoplankton and zooplankton dynamics; and dissolved oxygen balance (Figure 12).

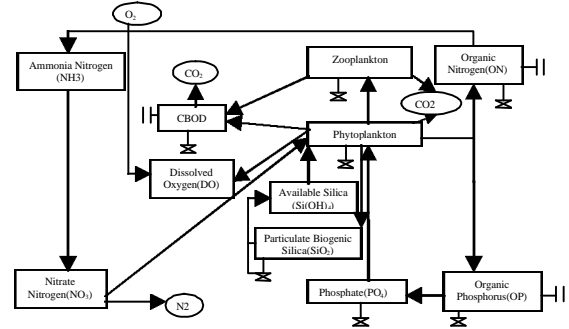


Figure 12. Schematic of interactions between nutrients, plankton and the dissolved oxygen balance.

The total of 13 state variables are considered as follows: ammonia (C_1), nitrate (C_2), phosphate (C_3), phytoplankton (C_4), carbonaceous biochemical oxygen demand (C_5), dissolve oxygen (C_6), organic nitrogen (C_7), organic phosphorus (C_8), zooplankton (C_9), coliform bacteria (C_{10}), total solids (C_{11}), available dissolved silica (C_{12}) and particulate biogenic silica (C_{13}). The interactions of the state variables are described mathematically as follows:

$$\frac{dC_1}{dt} = D_p a_{nc} (1 - f_{on}) C_4 + k_{71} \Theta_{71}^{T-20} C_7 \frac{C_4}{k_{mpc} + C_4} - k_{12} \Theta_{12}^{T-20} C_1 \frac{C_6}{k_{nit} + C_6} - G_p a_{nc} P_{NH3} C_4$$

+ death + mineralization - nitrification
- growth;

(4)

$$\frac{dC_2}{dt} = k_{12} \Theta_{12}^{T-20} C_1 \frac{C_6}{k_{nit} + C_6} - G_p a_{nc} (1 - P_{NH3}) C_4 - k_{2d} \Theta_{2d}^{T-20} C_2 \frac{k_{NO3}}{k_{NO3} + C_6}$$

+ nitrification - growth - denitrification;

$$\frac{dC_3}{dt} = D_p a_{pc} (1 - f_{op}) C_4 + k_{83} \Theta_{83}^{T-20} C_8 \frac{C_4}{k_{mpc} + C_4} - G_p a_{pc} C_4$$

+ death + mineralization - growth;

$$\frac{dC_4}{dt} = (G_p - D_p) C_4$$

+ growth - death;

$$\frac{d C_5}{d t} = a_{oc} k_{1D} C_4 + a_{oc} k_9 \Theta_9^{T-20} C_9 - k_D \Theta_D^{T-20} C_5 \frac{C_6}{k_{BOD} + C_6} - \frac{5}{4} \cdot \frac{32}{14} k_{2D} \Theta_{2D}^{T-20} C_2 \frac{k_{NO_3}}{k_{NO_3} + C_6}$$

+death +death - oxidation – denitrification;

$$\frac{d C_6}{d t} = k_a \Theta_a^{T-20} (C_{os} - C_6) + G_p \left(\frac{32}{12} + \frac{64}{14} a_{nc} (1 - P_{NH_3}) \right) C_4 - k_D \Theta_D^{T-20} C_5 \frac{C_6}{k_{BOD} + C_6} - \frac{64}{14} k_{12} \Theta_{12}^{T-20} C_1 \frac{C_6}{k_{nu} + C_6} - \frac{32}{12} k_{1R} \Theta_{1R}^{T-20} C_4$$

+aeration + growth - oxidation - nitrification -respiration;

$$\frac{d C_7}{d t} = D_p a_{nc} f_{on} C_4 - k_{71} \Theta_{71}^{T-20} C_7 \frac{C_4}{k_{mpc} + C_4}$$

+death –mineralization;

$$\frac{d C_8}{d t} = D_p a_{pc} f_{op} C_4 - k_{83} \Theta_{83}^{T-20} C_8 \frac{C_4}{k_{mpc} + C_4}$$

+death –mineralization;

$$\frac{d C_9}{d t} = (k_{1g} C_4 - k_9) \Theta_9^{T-20} C_9$$

+grazing – death;

$$\frac{d C_{10}}{d t} = -k_b \Theta_{10}^{T-20} C_{10}$$

- decay;

$$\frac{d C_{11}}{d t} = -T_{SS} C_{11} ;$$

$$\frac{d C_{12}}{d t} = c_{sc} (k_{fd} D_p - G_p) C_4 f_{dp} - a_{ex} (k_{dis} C_{12} - C_{13})$$

+death - growth – mineralization;

$$\frac{d C_{13}}{d t} = c_{sc} (1 - k_{fd}) D_p C_4 f_{dp} + a_{ex} (k_{dis} C_{12} - C_{13})$$

+death +mineralization.

Here $G_p = k_{1c} \cdot X_{RT} \cdot X_{RI} \cdot X_{RN}$ is phytoplankton growth rate; $X_{RT} = \theta_{1c}^{T-20}$ is temperature

adjustment factor; $X_{RI} = \frac{X_i}{I_s} \cdot \exp\left(-\frac{X_i}{I_s} + 1\right)^\beta$,

$X_i = I_{as} I_s \exp(-K_e \cdot z)$ xday, $\hat{\alpha}=0.1$;

is the light limitation factor as a function of average daily surface solar radiation I_{as} and saturating light intensity I_s , fraction day that is daylight f , depth z , total light extinction coefficient

K_e ; $X_{RN} = \min\left\{\frac{C_1 + C_2}{k_{mn} + C_1 + C_2}, \frac{C_3}{k_{mp} + C_3}\right\}$ is the

nutrient limitation factor as a function of dissolved inorganic phosphorus $DIP = C_3$ and nitrogen $DIN = C_1 + C_2$; $D_p = kr(T) + k_{1d} + k_{1g} \cdot C_9$ is reduction rate of phytoplankton;

$k_{1r}(T) = k_{1r}(20^\circ C) \cdot \theta_{1r}^{T-20}$ is endogenous respiration rate; k_{1d} = death rate representing the effect of parasitization; k_{1c} = grazing rate of phytoplankton per unit zooplankton population; C_9 = herbivorous zooplankton population grazing on phytoplankton.

Nutrient Dynamics. Nitrogen is returned from phytoplankton biomass pool to the organic nitrogen pools as a result of phytoplankton death, endogenous respiration and zooplankton grazing and mortality. Organic nitrogen undergoes settling, hydrolysis, mineralization and a bacterial decomposition and the end product is ammonia (NH_4-N) at a temperature – dependent rate. Ammonia nitrogen, in the presence of nitrifying bacteria and at a temperature and oxygen dependent rate, is then converted to (nitrification) nitrate (NO_3-N). Denitrification occurs under anaerobic conditions and CBOD decreases due to stabilization. Both NH_4 and $NO_2 + NO_3$ are available for phytoplankton uptake, however, the preferred form is NH_4-N for physiological reasons but it will utilize NO_3 for growth as NH_4 concentrations become depleted. The ammonia preference is described by a factor

$$P_{NH_3} = \frac{C_1}{k_{mn} + (C_2 + C_3)} \left(\frac{(C_2 + C_3)}{k_{mn} + C_1} + \frac{k_{mn}}{C_1 + (C_2 + C_3)} \right)$$

There is an adsorption-desorption interaction between dissolved inorganic phosphorus and dissolved particulate matter in the water column. The subsequent settling of the suspended solids together with the sorbed inorganic phosphorus can act as significant loss mechanism in the water column and is a source of phosphorus to the sediment.

Plankton Dynamics. Phytoplankton, the groups of free floating microorganisms, play a critical role in coastal marine ecosystems because they are the major source of energy for higher trophic levels and for driving nutrient cycles. They produce organic compounds and oxygen by consuming inorganic nutrient using light as energy source via photosynthesis. The phytoplankton growth relates to multiple factors, including available nutrients, water temperature, solar radiation, zooplankton grazing and tidal flushing. This model characterizes the aquatic plants as a whole by the total biomass of the phytoplankton present. So its maximum growth rate constant is adjusted throughout the simulation and described as $G_p = f(\text{temperature, light, nutrients})$.

It is assumed that phytoplankton population follows the Monod Growth Kinetics. Ambient light levels are a function of time of day, depth and self shading by phytoplankton themselves.

Phytoplankton losses include endogenous respiration, mortality, exudation, settling, parasitization and grazing by herbivorous zooplankton. Zooplankton kinetics depends primarily on grazing of phytoplankton and is reduced by mortality. When phytoplankton and zooplankton die, they form the organic carbon pool. A part of this carbon settled and other part is oxidized to oxygen by denitrification process.

Dissolved Oxygen Balance. Five state variables plays important role in the DO balance which are phytoplankton carbon, ammonia, nitrate, carbonaceous biochemical oxygen demand, and dissolved oxygen. The sources of oxygen are atmospheric reaeration and phytoplankton photosynthesis. DO saturation concentrations depend on salinity and temperature in tropical marine water. The reaeration rate coefficient is a function of the average water velocity, depth, wind, and temperature.

Total Suspended Solids and Fecal Coliform Bacteria Decay. In the model, TSS is modelled as a non-reactive material, with a settling velocity similar to that of particulate organic matter. In this respect, TSS can also be used as a conservative approach to predict the transport of non-reactive toxic pollutants. In the model, pathogens are indicated by fecal coliform bacteria, and are modelled as a first order decay reaction, with a decay rate constant (kb) of 10 day⁻¹.

Silica. The model incorporates two siliceous state variables, available (dissolved) silica and particulate biogenic silica. The silica cycle (Figure 12) is a major biogeochemical cycle in which diatom takes up available silica and recycle available and particulate biogenic silica through the action of metabolism and predation. A portion of the settled particulate biogenic silica dissolves within the sediments and returns to the water column as available silica by mineralization. The silica kinetics is represented by diatom production and metabolism, predation, Dissolution of particulate to dissolved silica which depends on alkalinity (higher in sea water), settling and exchange rate. Silica is very important state variable where diatoms biomass (40% of world phytoplankton) (Marine Botany, 1999) dominate ecosystem. Silica amounts limit the growth and behavior of diatoms. Diatoms have the ability to uptake silica, reducing it to very low concentration very rapidly. In open ocean, diatoms depend on transport of silicate-rich water from below the thermocline. The largest fluxes of silicate in the ocean's budget are driven by biological activity, potentially indicative of a system that can be biologically controlled. Because of their penchant

for aggregation and sinking, it plays an important role in the biological pump of carbon (20-25% of all organic carbon fixation by diatoms on the planet) (Marine Botany, 1999) to the deep ocean. Max Diatom cell counts of 554050 in 1965/1966 in Johore Straits (Chia, 1988) and of 35000 (approx.) in 2001 in Singapore Straits. So they have also been an indicator of water quality and pollution, as they are able to uptake and bind both organic and inorganic substances (pollutants).

Governing equations and numerical methodology. The mass conservation equation for dissolved constituents in the water column must account for all materials entering and leaving through direct and diffuse loading; advective and dispersive transport; and physical, chemical, and biological transformation. Consider the rectangular coordinate system with x- and y- coordinates are in the horizontal plane, and the vertical z- coordinate. The 3-D advective –diffusive equation with contaminant fluxes and the kinetic terms is described as follows:

$$\frac{\partial C}{\partial t} + \frac{\partial CU}{\partial x} + \frac{\partial CV}{\partial y} + \frac{\partial C(W-w)}{\partial z} - \frac{\partial}{\partial x} \left[E_x \frac{\partial C}{\partial x} \right] - \frac{\partial}{\partial y} \left[E_y \frac{\partial C}{\partial y} \right] - \frac{\partial}{\partial z} \left[E_z \frac{\partial C}{\partial z} \right] = \frac{Q(S-C)}{\Delta h \Delta x \Delta y} + R. \quad (5)$$

Here C is the concentration of N pollutants; S is the contamination of the liquid source with N pollutants; Q is the discharge of the liquid source; R is the chemical reaction description corresponding to the interaction equations for state variables; E_x, E_y, E_z are the turbulent eddy coefficients; w is the settling velocity; U, V, W are the currents velocity in x-, y-, and z- directions, respectively.

Model Calibration. Each utilized in the model kinetic coefficient is characterized by a certain range, depending on respective physical phenomenon. The coefficients may vary within these ranges according to local environmental conditions. Most of the kinetic coefficients were initially taken from the Potomac Estuary study by Thomann and Fitzpatrick (1982). Using baseline values of the state variables along with the analytical solution of the set of equations (4), majority of the coefficients were calibrated. Ambient light levels at different depths were calculated from extinction coefficients (Jayaraman, 2000).

The model was run using a horizontal grid of 1 km x 1 km, and a time step of 10 minutes. Two alternative types of contamination sources can be prescribed in the model:- $C=C_s$ and $dC/dt = C_s$. The vertical grid is non-uniform, based on output

from the hydrodynamics model. For this study the following layers were used: 0, 2.5m, 5m, 7.5m, 10m, 20m, 40m, 60m, 80m and 120m. Iterative runs were performed to fine-tune the kinetic coefficients into a final set of coefficients, which gave an equilibrium system response (Table 1).

Output results of nutrients, plankton, bacteria and suspended solids concentrations are analyzed as time series at selected locations at different depth or as spatial plots at selected times and depths. A typical model simulation run for a period of 30 days using above kinetic coefficients is obtained. In general, value of each state variable is fluctuating around the equilibrium state (baseline concentration). The period and amplitude of oscillations is due to combined effect of daily photosynthetic process and tidal forcing. The model is refined constantly as more field data become available. The computed values are compared against different sanitary criteria; including the safety of swimming beaches, and protection of coral reefs and aquaculture farms.

CONCLUSIONS

The hydrodynamic model is developed with emphasis on accurate description of all known regional phenomena, including previously neglected ones, such as accurate bathymetry, refined boundary conditions, as well as numerical incorporation of monsoons. Some of these considerations are presented in this paper, while further refinement is undergoing. More features would be added as data becomes available.

Simulations using NEUTRO model show that the model output is achieving baseline levels, and is able to reproduce the general features of the Singapore coastal waters. While the results presented in this paper are preliminary in nature, further calibration and validation of the model is going on as more field data become available. The ability of the model to predict the fate and transport of a number of nutrients, plankton, suspended solids and bacteria, makes it useful in the study of environmental impacts from coastal developments and discharges from outfalls. The model can be used to assist in the management and protection of Singapore's coastal water and the surrounding region.

ACKNOWLEDGEMENTS

The authors would like to thank Prof. Chan E.S., Dr. K.Gin Y H, for their helpful comments; Dr. M. Holmes; Dr. Zhang Q.Y. and to all TMSI people who helped in this research work.

APPENDIX

Table 1. Kinetic coefficients and other variables used in NEUTRO Model

a_{nc} = Nitrogen/carbon ratio = 0.25; f_{on} = Fraction of dead phytoplankton recycled to the organic nitrogen pool = 0.5; a_{pc} = Phosphorus/carbon ratio = 0.025; f_{op} = Fraction of dead phytoplankton recycled to the organic phosphorus pool = 0.5; k_{71} = Organic nitrogen mineralization rate = 1.15×10^{-8} 1/s; k_{12} = Nitrification rate = 1.66×10^{-7} 1/s; k_{2d} = Denitrification rate = 1.04×10^{-6} 1/s; k_{83} = Organic phosphorus mineralization rate = 2.15×10^{-9} 1/s; f_{d3} = Fraction of dissolved inorganic phosphorus in water column = 0.7; f_{d5} = Fraction of dissolved CBOD in water column = 0.5; f_{d7} = Fraction of dissolved organic nitrogen in water column = 0.8; f_{d8} = Fraction of dissolved organic phosphorus in water column = 0.8; k_{1r} = Endogenous respiration rate @ 20C = 0.7×10^{-7} 1/s; θ_{1r} = Temperature coefficient = 1.045; k_{1c} = Max specific growth rate @ 20C = 2.32×10^{-5} 1/s; k_{mn} = Half-saturation constant for nitrogen uptake = 25; k_{mp} = Half-saturation constant for phosphorus = 1; θ_c = Carbon/chlorophyll ratio = 30.0; θ_s = Temperature coefficient for SOD = 1.024; k_{1d} = Death rate for phytoplankton = 1.18×10^{-7} 1/s; DB = Non-algal extinction coefficient = 0.1 1/m; f = Fraction of day that is daytime = 0.5; sol = solar radiation = 483.2 ly/day; P_s = saturating light intensity = 200.0 ly/day; k_{1g} = Grazing rate of zooplankton = 1.00×10^{-6} 1/mg C/s; k_9 = Death rate for zooplankton = 1.16×10^{-7} 1/s; a_{oc} = Oxygen/carbon ratio = 2.67; k_{NO_3} = Half-saturation constant for oxygen limitation denitrification = 0.5; k_{BOD} = oxidation = 0.5 mg/l; k_{mpc} = Half-saturation constant for phytoplankton limitation of phosphorus recycling = 1.0; k_{nit} = half-saturation constant for oxygen limitation (nitrification) = 0.5 mg/l; k_d = Deoxygenation rate for CBOD = 2.47×10^{-7} 1/s; C_{sa} = Saturation concentration of dissolved oxygen = 5.5 mg/l; k_b = Bacteria decay rate = 11.57×10^{-5} 1/s.

REFERENCES

- Ambrose, B, Jr., T.A. Wool, and J.L. Martin. "The water quality analysis simulation program, WASP5; part a: model documentation," U.S. Environmental Protection Agency, Center for Exposure Assessment Modeling, Athens, GA, June, 1993
- Ambrose B., Wool T.A., Martin J.L., (2001) The Water Quality Analysis Simulation Program, WASP6, User Manual, US EPA, Athens, GA
- Andreas, M (1997), Modeling Primary Production in the North Sea, *Oceanography*, **10**, pp 24-26
- Baretta, J.W., Ruardij, P., Vested, H.J., Baretta-Bekker, J.G., 1994, Eutrophication modeling of the North Sea: two different approaches, *J. Ecological Modelling* 75/76, 471-483.
- Blumberg, A.f., and G.L. Mellor, 1987. A description of a three-dimensional coastal ocean circulation model. *Three-Dimensional Coastal Ocean Models*, vol.4, p.208, American Geophysical Union, Washington, D.C.

- Carl F. Cerco, Thomas Cole., 1995, User's Guide to the CE-QUAL-ICM Three – Dimensional Eutrophication Model (version 1), *US Army Corps of Engineer, Technical Report 95-15*.
- Carl F. Cerco and Thomas Cole (1993), Three-Dimensional, Eutrophication model of Chesapeake Bay, *Journal of Environmental Engineering*, 119, p 1007.
- Chao, X.B., Shankar, N.J. and Cheong, H.F., 1999. A three-dimensional multi-level turbulence model for tidal motion. *Ocean Engineering* 26, p.1023-1038.
- Cheong, H.F., Shankar, N.J. and Chan, C.T., 1992. Numerical modelling of tidal motion in southern waters of singapore. proceedings of the international conference on computer modelling for seas and coastal regions. Elsevier Applied Science, UK.
- Gin, K.Y.H. and Tklich, P. 1998. A three-dimensional eutrophication model for singapore costal water, *Environmental Strategies for the 21st century*: 280-286.
- Indonesia, Japan, Malaysia, Singapore, 1979. Report on the joint tidal and current studies in the straits of Malacca and Singapore.
- MINITAB Release 13.2 (2000), Minitab Inc., 3081 Enterprise Drive, State College, PA, U.S.A., <http://www.minitab.com>
- Kuusisto M., Jorma K., Juha S. (1998), Modelled Phytoplankton dynamics in the Gulf of Finland, *Environmental Modelling & Software*, 13, pp 461-470.
- Shankar, N.J., Cheong, H.F., Chan, C.T., 1997. Boundary fitted grid models for tidal motions in Singapore coastal waters. *Journal of Hydraulic Research* 35 (4), 47-60.
- Tham, A.K., 1953. A preliminary study of the physical, chemical and biological characteristics of singapore straits. London, Her Majesty's Stationery Office.
- Thomann, R.V. and Fitzpatrick, J.J. 1982. Calibration and verification of a model of the potomac estuary, 13. Hydroqual, Inc., Final Report to D.C. Dept. of Environmental services, Washington, D.C., 500pp.
- Zhang, H., and Chan, E.S., 1999. The physical characteristics of the water column in singapore straits. Proceeding of the Oceanology International 99, Pacific Rim, Exhibition and Conference.
- Zhang, Q.Y. 2000. A three-dimensional eutrophication model for singapore costal waters, PhD Thesis. National University of Singapore.
- Zhang, Q.Y. and Gin., K.Y.H., 2000. Three-dimensional numerical simulation for tidal motion in Singapore's coastal waters. *Coastal Engineering* 39, p.71-92.